Delft University of Technology

The Effects of Yaw and Sway Motion Cues in Curve Driving Simulation

Lakerveld, P.R.; Damveld, Herman; Pool, Daan; van der El, K.; van Paassen, Rene; Mulder, Max

Important note
To cite this publication, please use the final published version (if applicable).
Please check the document version above.

The Effects of Yaw and Sway Motion Cues in Curve Driving Simulation

P.R. Lakerveld, H.J. Damveld, D.M. Pool, K. van der El, M.M. van Paassen and M. Mulder *

* All authors are with the Control & Simulation Section, Faculty of Aerospace Engineering, Delft University of Technology, Delft, The Netherlands (Corresponding author: k.vanderel@tudelft.nl).

Abstract: This paper investigates the importance of yaw and sway motion cues in curve driving simulation. While such motion cues are known to enhance simulation realism, their function in supporting realistic driver behavior in simulators is still largely unknown. A human-in-the-loop curve driving experiment was performed in the SIMONA Research Simulator at TU Delft, in which eight participants were asked to follow a winding road's center-line, while being subject to wind disturbances. Four motion conditions were tested: 1) no motion, 2) yaw only, 3) sway only, and 4) both yaw and sway; each was tested with 5 m and 100 m road preview for correspondence with earlier work. Results show that visual road preview is essential for adequate road-following. Although the effects of yaw and sway cues are much smaller, sway motion feedback allows for improved disturbance-rejection performance, while yaw motion feedback results in reduced control activity. These distinctly different effects suggest that both motion cues are important for evoking realistic driving behavior in simulators.

Keywords: Driving simulation, driver behavior, motion cueing, curve driving.

1. INTRODUCTION

Driving simulators are an important tool in driver training, vehicle development and research related to automobile driving (Damveld et al., 2012; Berthoz et al., 2013). Compared to real driving, simulators provide a fully controllable environment that can be used to systematically investigate specific aspects of driving. In addition, simulators offer a cheap and safe alternative for real-world driver training or experiments.

Unfortunately, simulators are typically unable to reproduce the complete vestibular sensations experienced during real driving. Especially curve driving poses a challenge (Berthoz et al., 2013), as the turning of the vehicle induces strong and prolonged specific forces, which demand a large motion workspace. Negotiating a curve, a driver experiences both a turning sensation due to the vehicle's yaw motion, and a centrifugal sensation (being pushed to the side) due to linear sway accelerations. To perform a valid trade-off between motion system costs and driving simulators' ability to support realistic driving behavior, it is important to know to what extent these different cues affect drivers in their task.

It is generally acknowledged that yaw and sway motion cues help drivers negotiating curves (Reymond et al., 2001). While driving on a straight road (Repa et al., 1981), or during a lane change (Greenberg et al., 2003) with random crosswinds, the availability of motion cues has been found to result in smaller heading and lateral position errors. The driver's reaction time can decrease significantly when motion feedback is present (Wierwille et al., 1983). In addition, yaw and sway motion cues also affect drivers'

longitudinal control behavior, for example, in helping to reduce forward velocity in curved road sections (Reymond et al., 2001; Valente Pais et al., 2009). However, for curve driving the effects of the perceivable yaw and sway cues on driver behavior are still largely unclear.

This paper aims to quantify how yaw and sway motion cues affect driver steering behavior. To do so, a curve driving experiment was performed in the SIMONA Research Simulator at TU Delft, in which eight participants performed a simplified constant-velocity curve driving task. Participants performed this task with four different motion cueing settings: 1) no motion, 2) only yaw motion, 3) only sway motion, and 4) both yaw and sway motion. To tie in with earlier work (Damveld et al., 2015), all motion conditions were performed with 5 m and with 100 m of visual preview of the line representing the driving lane's center, resulting in a total of eight conditions. Different objective performance and control activity measures were calculated to detect the individual and combined effects of yaw and sway motion on driver steering behavior.

This paper starts with some background on curve driving and drivers' motion perception. Then, the details of the experiment are presented, followed by its results. The paper ends with a discussion and our main conclusions.

2. BACKGROUND

2.1 The Human in a Curve Driving Task

Lateral vehicle control involves a driver continuously guiding a vehicle along a (possibly curved) road, while attenuating disturbances such as wind gusts (see Fig. 1). It

requires the human driver to close two nested feedback loops: an inner loop to control the vehicle's heading ψ, and an outer loop to control its lateral position on the road y. To do so, the driver integrates multimodal information perceived from the environment, the most important of which are the visual and the vestibular channels (Gum, 1973). The vehicle state (i.e., position, heading and their derivatives) is perceived relative to the road curvature through the visual system. The driver can typically see the road ahead, which is referred to as *preview*. Sivak (1996) and Damveld et al. (2015), amongst others, showed that this visual preview information supports "normal" curve driving behavior, by allowing drivers to see, and anticipate, the road's upcoming track. The vestibular organ provides drivers with further yaw and sway motion (velocity/acceleration) information through the semicircular canals and the otoliths, respectively (Gum, 1973).

One of first mathematical models proposed for modeling human curve driving was developed by McRuer et al. (1977). Fig. 2 shows a slightly adapted block diagram for this model as used by Damveld et al. (2012) in a more recent study. Despite the fact that this model only accounts for drivers' responses to visual information – and thus lacks an explicit vestibular modality – the curve driving task analyzed in this paper is still defined as prescribed by the model of Fig. 2. The model shows that only the vehicle's ψ and y degrees-of-freedom are considered. Furthermore, a curve driving task at a fixed forward velocity U_0 is considered; for our experiment $U_0 = 13.9$ m/s (50 km/h). The vehicle's heading dynamics G_δ^ψ and the lateral slip dynamics G_δ^v are given by:

$$G_\delta^\psi(s) = \frac{73.6s + 883.1}{s^3 + 24.19s^2 + 146.2s}, \tag{1}$$

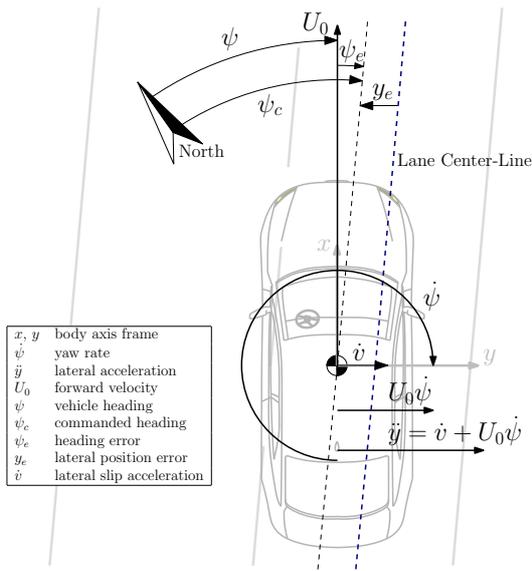$$G_\delta^v(s) = \frac{100.0s + 196.4}{s^2 + 24.19s + 146.2}. \tag{2}$$

Fig. 1. A schematic representation of lateral vehicle control kinematics during road following.

The driver's control output δ_s (steering wheel angle) is directly proportional to the front wheel angle δ_f, with a steering-wheel ratio of $G_s = 1/17$.

McRuer et al. (1977)'s driver model (Fig. 2) clearly shows the driver's hypothesized heading and lateral position feedback loops. The response to the previewed road ahead is incorporated through the feedforward block, $K_r Y_{p_i}$, with the commanded heading ψ_c as input. Because the vehicle dynamics are generally second-order integrator systems, drivers have to generate some lead ($T_L s + 1$) in the inner loop of their control response to obtain favorable closed-loop behavior (McRuer et al., 1977). Motion feedback is known to help human controllers when they control systems with such dynamics (Shirley and Young, 1968; Jex et al., 1978), as the vestibular system, in parallel to the visual system, can provide them the required lead.

2.2 Analysis of Motion Feedback

During curve driving, drivers perceive physical motion through the vestibular organ: the semicircular canals (sc) are sensitive to yaw accelerations $\ddot{\psi}$, and the otholits (oto) are sensitive to lateral accelerations, $\ddot{y} (= \dot{v} + U_0\dot{\psi})$. The information m perceived by the driver is subject to each organ's dynamics H and a perception delay τ_m. Replacing the derivatives with the Laplace operator s, m can be written in the frequency domain as

$$M_{oto}(s) = H_{oto}(s)e^{-\tau_m s}s^2 Y(s)$$
$$= H_{oto}(s)e^{-\tau_m s}(sV(s) + U_0 s\Psi(s)), \tag{3}$$
$$M_{sc}(s) = H_{sc}(s)e^{-\tau_m s}s^2\Psi(s). \tag{4}$$

Capitals indicate the Fourier transforms of the respective signals. Hosman (1996) describes two well-known models for the otolith and semicircular canal dynamics, respectively:

$$H_{oto}(s) = \frac{0.057(1+s)}{(1+0.5s)(1+0.016s)}, \tag{5}$$

$$H_{sc}(s) = \frac{5.95(1+0.11s)}{(1+5.9s)(1+0.005s)}. \tag{6}$$

For our application, two simplifications are possible, i.e.:

- $\dot{v} << U_0\dot{\psi}$ for a forward velocity of $U_0 = 13.9$ m/s (as used in our experiment), so the lateral acceleration in (3) can be approximated by just the centripetal acceleration, $\ddot{y} \approx U_0\dot{\psi}$;
- In the frequency range of interest, 0.1-10 rad/s, the vestibular organ dynamics can be approximated by $H_{oto}(s) \approx K_{oto}$ and $H_{sc}(s) \approx \frac{K_{sc}}{s}$.

Substitution of these simplifications in (3) and (4) yields:

$$M_{oto}(s) \approx K_{oto}e^{-\tau_m s}U_0 s\Psi(s), \tag{7}$$

$$M_{sc}(s) \approx \frac{K_{sc}}{s}e^{-\tau_m s}s^2\Psi(s)$$
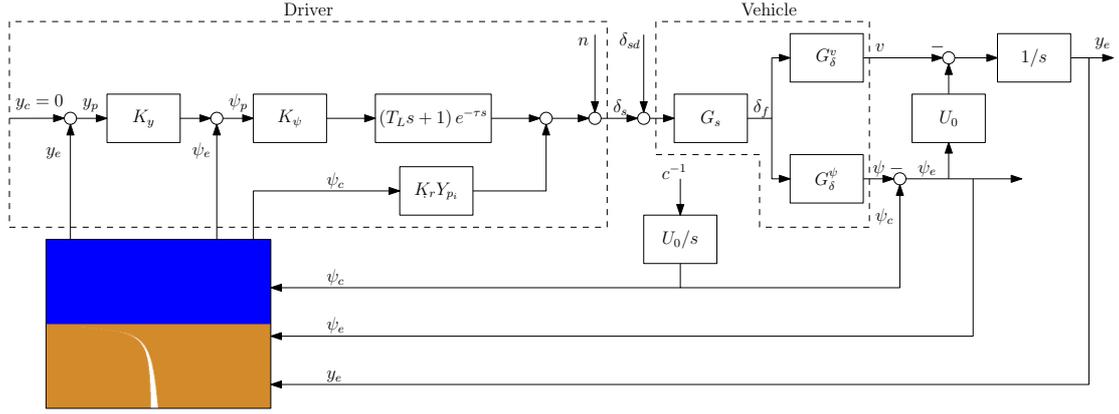$$\approx K_{sc}e^{-\tau_m s}s\Psi(s). \tag{8}$$

Fig. 2. A driver model for curve negotiation based on only visual feedback, adapted from (Damveld et al., 2012).

Eq. (7) and (8) show that both yaw and sway motion feedback can effectively provide yaw rate information (lead) to the driver. As such, it may be expected that driver steering behavior is similarly affected by the presence of both individual cues, as well as when they are presented simultaneously (redundancy).

3. METHOD

3.1 Apparatus

A human-in-the-loop experiment was performed in the SIMONA Research Simulator at TU Delft. This simulator has a six degree-of-freedom hydraulic hexapod motion system, which can provide a maximum yaw rotation of $\pm 41.6°$ and a maximum sway translation of ± 1.031 m (Berkouwer et al., 2005). Outside visual scenes can be presented using the simulator's collimated projection system, providing a $180° \times 40°$ field of view. Drivers gave steering inputs with an aircraft yoke, as the simulator was not yet equipped with a steering wheel at the time of the experiment.

3.2 Independent Variables

The effects of three independent variables on driver steering behavior were tested: yaw motion, sway motion, and visual preview distance. The yaw and sway cues both had two levels: a control condition without any motion feedback, and a condition with the maximum motion feedback possible in the SIMONA simulator. Because the effect of visual preview on driver steering is substantial (Sivak, 1996; Damveld et al., 2015), all motion settings were tested with 5 m and 100 m of preview. With 100 m of preview a large part of the track ahead is visible (see Fig. 3), so drivers can rely more heavily on feedforward control. This is more difficult when only 5 m preview is available; therefore, here, the effects of motion feedback may be more pronounced. The full factorial of the three independent variables was tested, yielding a total of eight conditions.

3.3 Control Variables

The important control variables of the experiment comprise the visual scene and road presentation, the motion cueing settings, and the steering wheel disturbance and the road trajectory to be followed. The vehicle dynamics and its fixed forward velocity were already given in Section 2.1.

In the simplified visual scene used in the experiment, depicted in Fig. 3, only the driving lane's center-line is shown. This results in participants truly attempting to track the lane center ("tracking") instead of simply trying to adequately keep the lane ("boundary-avoidance"), which strongly reduces the natural variability in driver steering behavior and thus yields more consistent measurements. To eliminate effects of optic flow, no other visual information or texturing is shown besides a continuous horizon line. As such, visual yaw rate information is minimized.

Due to the limited workspace of the SIMONA simulator's hexapod motion system, it was impossible to present yaw and sway motion cues as perceived during real curve driving. The issue with cueing such car driving on a hexapod are the sustained lateral accelerations, which require significantly more simulator travel than typically available (Berthoz et al., 2013). A frequently used strategy for limiting the simulator's travel is by high-pass filtering the vehicle motion. The third-order high-pass filter applied in our experiment is given by:

$$G_{mf}(s) = K_{mf} \frac{s^2}{s^2 + 2\zeta_n \omega_n s + \omega_n^2} \frac{s}{s + \omega_b}. \qquad (9)$$

In (9), K_{mf} indicates the filter gain, ω_n and ζ_n the second-order filter break frequency and damping ratio, respectively, and ω_b the first-order filter break frequency.

For fair comparison of the effects of both cues, we chose to apply identical filters for the yaw and sway motion. However, both cues were scaled (with a different gain) relative to the semicircular canal and the otolith perception thresholds to equalize the information in each channel. First, sway feedback was maximized with respect to the available motion space, as sway cueing is most limited
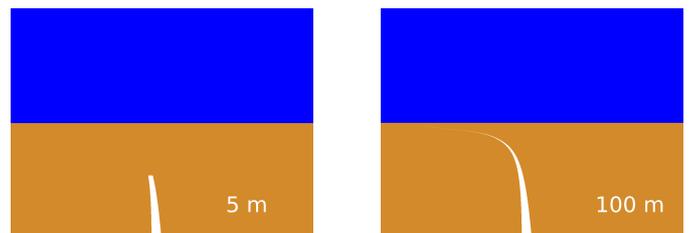

Fig. 3. Outside visual during the experiment

Table 1. Input signals' parameters: commanded heading ψ_c and steering wheel disturbance δ_{sd}.

k [-]	n_k [-]	ω_k [rad/s]	A_k [rad]	φ_{k_1} [rad]	φ_{k_2} [rad]	φ_{k_3} [rad]	φ_{k_4} [rad]	φ_{k_5} [rad]	n [-]	ω_k [rad/s]	A_k [rad]	φ_{k_1} [rad]	φ_{k_2} [rad]	φ_{k_3} [rad]	φ_{k_4} [rad]	φ_{k_5} [rad]
			commanded heading ψ_c									steering wheel disturbance δ_{sd}				
1	2	0.127	0.531	3.640	2.237	3.083	1.419	1.419	4	0.251	0.036	1.498	0.320	0.950	-0.240	-0.589
2	3	0.188	0.354	3.931	2.398	3.796	2.537	2.725	5	0.314	0.036	2.394	1.600	2.076	1.846	2.899
3	7	0.440	0.152	3.999	2.680	2.915	1.134	2.379	9	0.566	0.036	0.406	-1.225	-0.727	0.693	-1.233
4	8	0.503	0.133	-1.348	2.487	3.727	3.951	-1.490	10	0.628	0.036	1.849	1.245	0.306	0.173	1.721
5	19	1.194	0.054	-0.026	4.060	-0.136	-0.106	4.407	21	1.320	0.036	2.418	-2.584	-2.418	2.284	-3.046
6	20	1.257	0.051	0.348	0.455	0.622	-0.761	0.470	22	1.382	0.036	-0.706	-0.898	-1.988	3.140	-1.467
7	47	2.953	0.018	0.981	2.152	2.163	1.360	1.169	49	3.079	0.036	1.512	-0.991	0.329	0.365	-0.757
8	48	3.016	0.018	2.252	4.177	3.762	-1.150	-0.982	50	3.142	0.036	0.888	0.840	1.563	0.937	2.481
9	99	6.220	0.003	-0.863	-0.030	4.154	3.499	3.916	101	6.346	0.018	2.509	2.131	-2.700	2.382	2.826
10	100	6.283	0.003	0.250	-1.386	1.372	0.516	1.179	102	6.409	0.018	-2.234	-2.216	2.875	-2.275	-1.949

in a hexapod simulator. This gave the following sway cueing settings: $\zeta_n = 0.7$, $\omega_n = 0.7$ rad/s, $\omega_b = 0.5$ rad/s, $K_{mf} = 0.2$. The yaw gain was then determined from the ratio of human perception thresholds for yaw and sway, $\dot{\psi}_{thr} = 0.0166$ (Heerspink et al., 2005) and $\ddot{y}_{thr} = 0.0850$ m/s^2 (Hosman, 1996), respectively. With the simplified vehicle kinematics from Section 2.2 (i.e., $\ddot{y} \approx U_0\dot{\psi}$), and a forward velocity of 13.9 m/s, it follows that the yaw gain should be about 2.7 times higher than the sway gain. Therefore, K_{mf} was set to 0.55 for yaw.

The road to be followed, defined by the commanded heading ψ_c, was constructed as a sum of 10 sinusoids:

$$\psi_c(t) = \sum_{k=1}^{10} A_k \sin\left(\omega_k t + \varphi_k\right) \tag{10}$$

The frequencies ω_k, amplitudes A_k and phases φ_k are provided in Table 1. The frequencies were integer multiples n_k of the base frequency $\omega_0 = 0.0628$ rad/s, which corresponds to a measurement time $T = 100$ s. The steering wheel disturbance signal was constructed equivalently (see Table 1). The commanded heading and steering wheel disturbance signals had a total power of 0.2271 rad^2 and 0.0055 rad^2, respectively. Five different realizations of the signals were used and presented in random order, so participants could not memorize them. The different signal realizations only differed by their sinusoids' phases φ_k.

3.4 Dependent Measures

During the experiment the heading angle error ψ_e, the lateral deviation y_e, and the steering wheel input δ_s were recorded. From these quantities, two steering performance measures were calculated, namely the heading error variance $\sigma^2(\psi_e)$ and the lateral position error variance $\sigma^2(y_e)$. Additionally, the control variance $\sigma^2(\delta_s)$ was calculated as a measure for the driver's control activity. The variances were also separated into target tracking, disturbance rejection, and remnant contributions in the frequency domain, as in (Jex et al., 1978).

3.5 Participants and Experiment Procedure

Eight motivated subjects participated in the experiment. Their average age was 24.1 years with a standard deviation of 1.6 years, while their driving experience ranged from 0.5 to 8 years, and from 500 to 8000 km per year. The participants were instructed to follow the target line (i.e., the road center) as accurately as possible.

The experiment started with a training session of approximately 45 minutes, during which the participant performed all eight conditions twice. Then, the actual measurements were started. Five consecutive runs were performed for each condition, after which the participant moved on to the next condition. After each run, the participants were informed of their performance, to further motivate them. In-between each set of two or three conditions a 15 minute break was taken, resulting in a total experiment duration of approximately four hours.

3.6 Experiment Design and Data Analysis

A Latin-square experimental design was used to cancel out any effects of fatigue and training during the experiment. For each condition, the participants tracked signals of all five different realizations of the target and disturbance, of which the final three were used in the data analysis. Performance and control variances were calculated for each particular measurement run, after which the variances were averaged over the three measurement runs per subject. To test for statistical significant effects, a repeated-measures analysis of variance (ANOVA) was used. The Kolmogorov-Smirnov test was applied to check the normality of all tested samples.

3.7 Hypotheses

Based on the observation that both yaw and sway motion cues provide the driver with information of the vehicle's yaw rate (see Section 2.2), and that the vehicle dynamics require the driver to generate lead, we formulated the following hypotheses:

(1) Compared to no motion feedback, separate yaw or sway motion will result in a similar improvement of driver performance, as characterized by a reduction in $\sigma^2(\psi_e)$ and $\sigma^2(y_e)$;
(2) Compared to no motion feedback, separate yaw or sway motion will cause a similar decrease in control activity. This is characterized by a drop in $\sigma^2(\delta_s)$, and is an effect typically found in target-tracking tasks (Hosman, 1996; Pool et al., 2008);
(3) When yaw motion is available, no significant change in performance and control activity occurs when sway motion is added, and vice versa.

4. RESULTS

The calculated steering performance and control activity measures are shown in Fig. 4, while Table 2 shows the results of the corresponding ANOVAs. As is clear from Fig. 4, the effect of preview is most notable; both the heading and lateral position error decrease markedly when 100 m road preview is available, especially the target
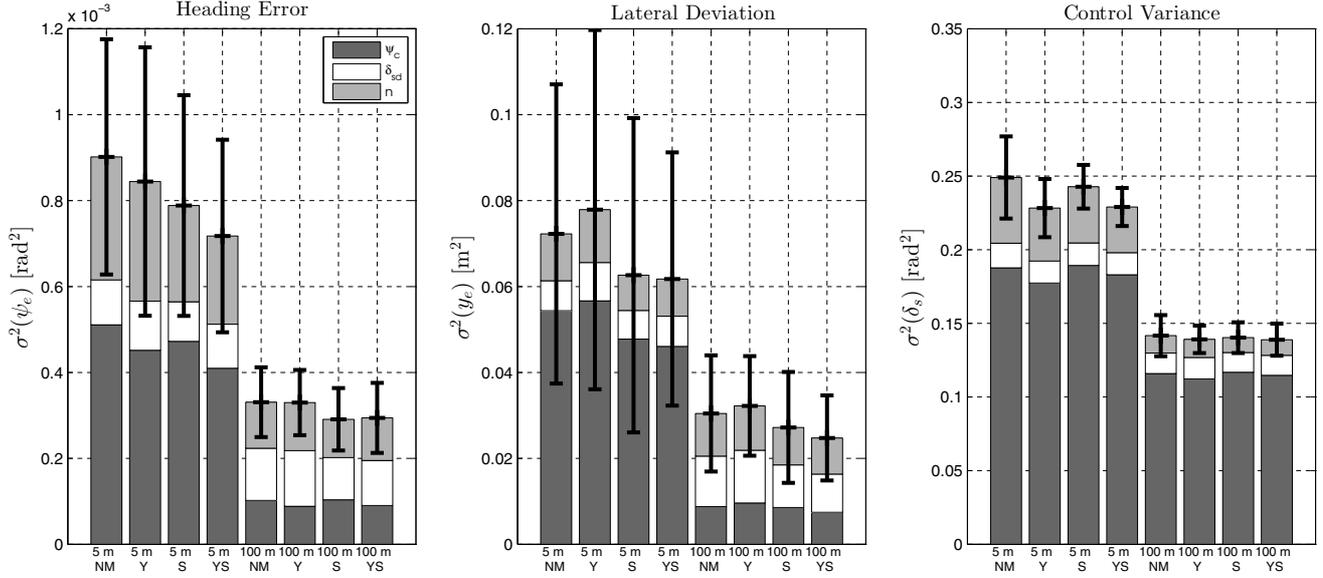
Fig. 4. Variance of the heading error ψ_e, the lateral deviation y_e, and control input δ_s, with the 95% confidence intervals. The contributions of the target ψ_c, disturbance δ_{sd}, and remnant n are separately indicated.

Table 2. Repeated measures ANOVA results of performance measures and control activity

independent variable	dependent variable																
	$\sigma^2(\psi_e)$		$\sigma^2(\psi_{e_{\psi_c}})$		$\sigma^2(\psi_{e_{\delta_{sd}}})$		$\sigma^2(y_e)$		$\sigma^2(y_{e_{\psi_c}})$		$\sigma^2(y_{e_{\delta_{sd}}})$		$\sigma^2(\delta_s)$		$\sigma^2(\delta_{s_{\psi_c}})$		$\sigma^2(\delta_{s_{\delta_{sd}}})$
factor	F	sig.	F	sig.	F	sig.	F	sig.	F	sig.	F	sig.	F	sig.	F	sig.	F	sig.
preview	37.2	**	32.3	**	3.9	-	15.7	**	16.7	**	17.6	**	202.2	**	366.6	**	8.6	*
yaw	1.8	-	3.1	-	2.0	-	0.1	-	0.0	-	0.7	-	7.8	*	16.2	**	0.3	-
sway	4.4	-	0.5	-	29.0	**	2.4	-	1.1	-	7.1	*	0.1	-	1.4	-	1.7	-
P × Y	2.7	-	2.0	-	0.3	-	0.2	-	0.0	-	2.8	-	7.4	*	12.1	*	2.0	-
P × S	2.8	-	1.0	-	1.8	-	0.5	-	0.6	-	0.7	-	0.1	-	0.3	-	0.0	-
Y × S	0.0	-	0.0	-	0.0	-	0.9	-	0.6	-	1.9	-	1.1	-	2.8	-	0.2	-
P × Y × S	0.1	-	0.0	-	0.0	-	0.1	-	0.1	-	0.0	-	0.4	-	0.7	-	0.9	-

** is significant (p < 0.01), * is significant (p < 0.05), - is not significant (p ≥ 0.05)

tracking component (ψ_c). However, disturbance-rejection performance degrades slightly, as indicated by a larger heading error $\psi_{e_{\delta_{sd}}}$ (insignificant effect, Table 2), and lateral position error $y_{e_{\delta_{sd}}}$ (significant effect). These trends suggest that drivers give less priority to disturbance-rejection when preview is available. Furthermore, control activity is significantly lower with 100 m preview, again mainly attributable to the target component.

The effects of the yaw and sway motion cues are generally smaller. Nonetheless, Fig. 4 shows that the presence of yaw motion consistently induces a lower control activity, specifically in target tracking (significant effect). This effect appears to be stronger when 5 m preview is available (Fig. 4), and indeed, the ANOVA results reveal a significant interaction effect between preview and yaw.

Yaw and sway motion cues had no significant effect on the total performance measures, nor on the target-tracking part of the task. For clarity, the disturbance-rejection performance (white bars in Fig. 4) is plotted separately in Fig. 5. This shows that sway motion feedback generally results in better disturbance-rejection performance (significant effect), but that it slightly deteriorates with yaw motion feedback (insignificant effect). When sway motion is added when yaw is already available, both performance measures consistently improve, suggesting different roles of both cues on drivers' steering performance.

5. DISCUSSION

Based on an analytic analysis of curve driving kinematics, it was hypothesized that both yaw and sway motion feedback would induce a similar effect on driver steering behavior during curve driving. This was contradicted by our measurements, as sway motion feedback resulted in an improved disturbance-rejection performance, while yaw motion feedback induced a lower control activity. This suggests that yaw and sway motion have a distinctly different effect on human curve driving behavior, and that both cues are important for high-fidelity driving simulation. However, the measured effect of road preview
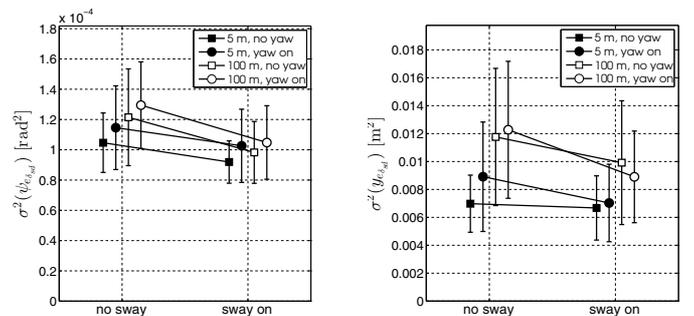

Fig. 5. Disturbance-rejection performance, with 95% confidence intervals.

was much larger than the effects of both vestibular cues, confirming that driving is primarily a visual task (Sivak, 1996; Damveld et al., 2015).

Our analytic analysis that yaw and sway motion cues provide the driver with similar information, hence evoke similar driver steering behavior, was clearly wrong. In future research, the assumptions made in this analysis should be critically reviewed; for instance, by using a true perception model, and by accounting for the full vestibular system dynamics ((5) and (6)) in the relative perception threshold calculation. Moreover, our hexapod simulator provided drivers with reduced motion cues; to validate our results it is recommended to repeat the experiment in a simulator with a larger motion space, which can provide the actual motion cues experienced in curve driving. In addition, our results would gain value if they can be reproduced for a more general population (e.g., older aged subjects).

Finally, enhanced understanding of the role of motion feedback on human curve driving behavior may be obtained from a more thorough analysis of our data. An approach using system identification and parameter estimation techniques in combination with a mathematical driver model (as briefly introduced in this paper) (Damveld et al., 2015) seems promising, as this allows for deeper insights in driver's underlying control mechanisms. To do so, first, drivers' use of motion feedback should be incorporated in a driver model, while inclusion of the latest findings on their use of the dominant visual preview cue is also desirable (Damveld et al., 2015; Van der El et al., 2015).

6. CONCLUSION

In this paper, the individual effects of yaw and sway motion feedback on driver steering behavior were investigated, in tasks with and without visual preview of the road's center-line ahead. We performed a curve driving experiment in a moving-base simulator. Results show that the effects of both motion cues are small compared to the presence of visual preview information. Sway motion feedback helps to improve disturbance-rejection performance, without a notable difference in control activity. With yaw motion feedback the control activity is lower, but task performance is not improved. Both yaw and sway motion feedback appear to be important cues in curve driving tasks, which are essential for evoking realistic curve driving behavior in simulators.

REFERENCES

Berkouwer, W.R., Stroosma, O., Van Paassen, M.M., Mulder, M., and Mulder, J.A. (2005). Measuring the performance of the SIMONA research simulator's motion system. In *Proceedings of the AIAA Modeling and Simulation Technologies Conference, San Francisco (CA)*.

Berthoz, A., Bles, W., Bülthoff, H.H., Correia Grácio, B.J., Feenstra, P., Filliard, N., Hühne, R., Kemeny, A., Mayrhofer, M., Mulder, M., Nusseck, H.G., Pretto, P., Reymond, G., Schlüsselberger, R., Schwandter, J., Teufel, H.J., Vailleau, B., van Paassen, M.M., Vidal, M., and Wentink, M. (2013). Motion Scaling for High-Performance Driving Simulators. *IEEE Transactions on Human-Machine Systems*, 43(3), 265–276.

Damveld, H.J., Steen, J., Happee, R., Van Paassen, M.M., and Mulder, M. (2015). Investigating the effect of preview distance on driver steering behavior using system identification. *IEEE Transactions on Systems, Man and Cybernetics*. Submitted.

Damveld, H.J., Wentink, M., van Leeuwen, P.M., and Happee, R. (2012). Effects of Motion Cueing on Curve Driving. In *Proceedings of the Driving Simulation Conference 2012*.

Greenberg, J., Artz, B., and Cathey, L. (2003). The effect of lateral motion cues during simulated driving. In *DSC North America 2003 Proceedings*.

Gum, D.R. (1973). Modeling of the human force and motion-sensing mechanisms. Technical report, Air Force Human Resources Laboratory.

Heerspink, H.M., Berkouwer, W.R., Stroosma, O., and Mulder, M. (2005). Evaluation of vestibular thresholds for motion detection in the simona research simulator. In *Proceedings of the AIAA Modeling and Simulation Technologies Conference*.

Hosman, R.J.A.W. (1996). *Pilots Perception and Control of Aircraft Motions*. Ph.D. thesis, Delft University of Technology.

Jex, H.R., Magdaleno, R.E., and Junker, A.M. (1978). Roll tracking effects of g-vector tilt and various types of motion washout. In *Proceedings of the Fourteenth Annual Conference on Manual Control*, 463–502.

McRuer, D.T., Allen, R.W., Weir, D.H., and Klein, R.H. (1977). New results in driver steering control models. *Human Factors*, 19(4), 381–397.

Pool, D.M., Mulder, M., Van Paassen, M.M., and Van der Vaart, J.C. (2008). Effects of peripheral visual and physical motion cues in roll-axis tracking tasks. *Journal of Guidance, Control, and Dynamics*, 31(6), 1608–1622.

Repa, B.S., Leucht, P.M., and Wierwille, W.W. (1981). The influene of motion cues on driver-vehicle performance in a simulator. In *Proceedings of the Seventeenth Annual Conference on Manual Control*.

Reymond, G., Kemeny, A., Droulez, J., and Berthoz, A. (2001). Role of lateral acceleration in curve driving: Driver model and experiments on a real vehicle and a driving simulator. *Human Factors*, 43(3), 483–495.

Shirley, R.S. and Young, L.R. (1968). Motion Cues in Man-Vehicle Control – Effects of Roll-Motion Cues on Human Operator's Behavior in Compensatory Systems with Disturbance Inputs. *IEEE Transactions on Man-Machine Systems*, 9(4), 121–128.

Sivak, M. (1996). The information that drivers use: Is it indeed 90% visual? *Perception*, 25(9), 1081–1089.

Valente Pais, A.R., Wentink, M., Van Paassen, M.M., and Mulder, M. (2009). Comparison of three motion cueing algorithms for curve driving in an urban environment. *Presence: Teleoperators and Virtual Environments*, 18(3), 200–221.

Van der El, K., Pool, D.M., Damveld, H.J., Van Paassen, M.M., and Mulder, M. (2015). An empirical human controller model for preview tracking tasks. *IEEE Trans. on Cybernetics*, accepted, online preprint available.

Wierwille, W.W., Casali, J.G., and Repa, B.S. (1983). Driver steering reaction time to abrupt-onset crosswinds, as measured in a moving-base driving simulator. *Human Factors*, 25(1), 103–116.